

# A comprehensive and easy-to-use multi-domain multi-task medical imaging meta-dataset (MedIMeta)

Stefano Woerner<sup>1</sup>, Arthur Jaques<sup>1</sup>, and Christian F. Baumgartner<sup>1,2</sup>

<sup>1</sup>Cluster of Excellence “Machine Learning: New Perspectives for Science”, University of Tübingen, Germany

<sup>2</sup>Faculty of Health Sciences and Medicine, University of Lucerne, Switzerland

## ABSTRACT

While the field of medical image analysis has undergone a transformative shift with the integration of machine learning techniques, the main challenge of these techniques is often the scarcity of large, diverse, and well-annotated datasets. Medical images vary in format, size, and other parameters and therefore require extensive preprocessing and standardization, for usage in machine learning. Addressing these challenges, we introduce the Medical Imaging Meta-Dataset (MedIMeta), a novel multi-domain, multi-task meta-dataset. MedIMeta contains 19 medical imaging datasets spanning 10 different domains and encompassing 54 distinct medical tasks, all of which are standardized to the same format and readily usable in PyTorch or other ML frameworks. We perform a technical validation of MedIMeta, demonstrating its utility through fully supervised and cross-domain few-shot learning baselines.

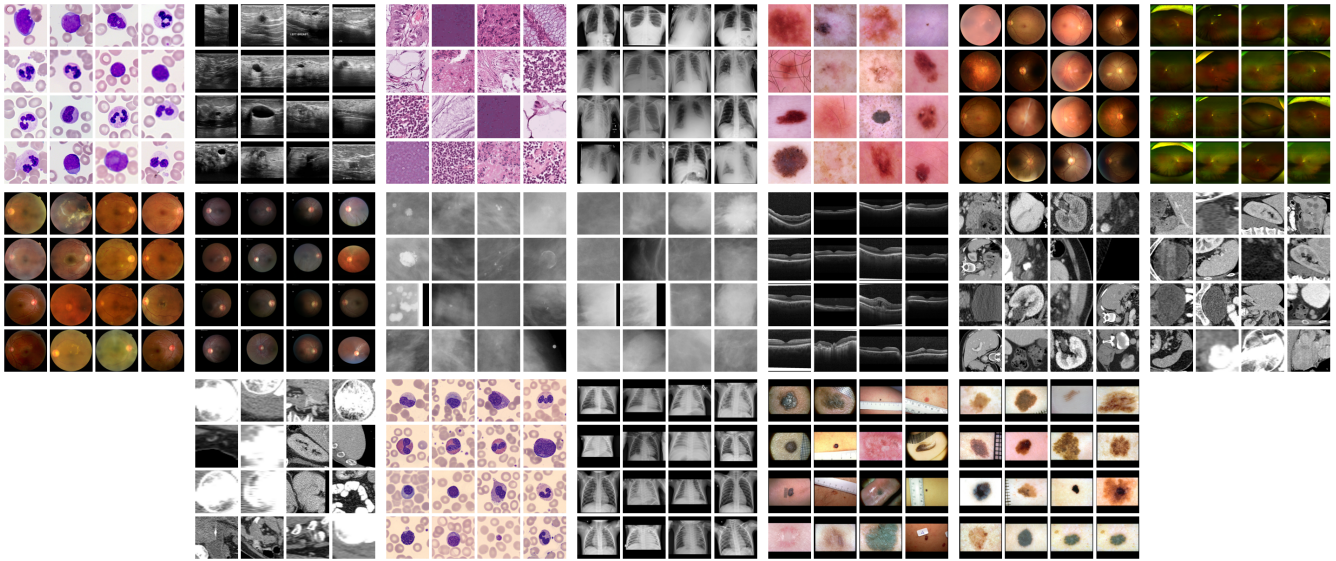


**Figure 1.** Example images of all MedIMeta datasets.

## Background & Summary

In recent years, the field of medical image analysis has undergone a transformative shift with the integration of machine learning (ML) techniques fundamentally expanding the landscape of diagnostic and therapeutic strategies. The advancement of this field hinges on the availability of large, diverse, and well-annotated datasets, which are pivotal for training robust and effective ML models. However, the process of collecting raw medical images and bringing them to a format suitable for ML applications is often complex and fraught with challenges. Medical images vary in format, size, and other parameters and therefore require extensive preprocessing and standardization, a task that becomes increasingly complex when working with multiple datasets from multiple domains that need to be integrated into a cohesive standardised format.

Another challenge is the scarcity of annotated datasets in medical imaging, particularly for rare diseases or specific conditions. This limitation has sparked the exploration of few-shot learning (FSL) methodologies. These try to learn from few

examples and are designed to make predictions based on a limited number of training examples. While humans are adept at learning and making accurate predictions from minimal information, achieving comparable levels of performance in machines remains a significant challenge.

Cross-domain few-shot learning (CD-FSL) allows models to leverage the information learned for a task in one domain and apply it to another task in another domain, potentially reducing the need for extensive data in every new task. This ability is of immense value in these contexts, especially for rare conditions. We define a domain as a particular type of subject, i.e. the studied anatomical region in the medical context, combined with a particular imaging modality. Despite its potential, the cross-domain transfer poses significant challenges, given the inherent variability in imaging modalities, disease presentations, and data characteristics across different medical fields and clinics. In addition to the variability in domains, the nature of tasks involved in medical image analysis varies considerably, encompassing a range of classification types such as binary, multi-class, or multi-label, and differing in the number of target labels or classes. Developing algorithms capable of navigating these complexities is essential for effective knowledge transfer. In order to facilitate the development of such algorithms, good preprocessing and standardization across the different domains are even more critical in this context.

Addressing these challenges, we introduce the Medical Imaging Meta-Dataset (MedIMeta), a novel multi-domain, multi-task meta-dataset designed to facilitate the development and standardized evaluation of ML models and cross-domain FSL algorithms for medical image classification. MedIMeta contains 19 medical imaging datasets spanning 10 different domains and encompassing 54 distinct medical tasks, offering opportunities for both single-task and multi-task training. Many of the tasks are diagnostic tasks or are tasks immediately relevant to a diagnosis. Additionally, MedIMeta contains auxiliary tasks (such as gender prediction) that may not have immediate clinical relevance but may nevertheless be of interest. Furthermore, they have relevance for multi-task training or for training FSL algorithms which benefit from having a large amount of tasks.

For improved practicality, each dataset within the MedIMeta dataset is standardized to a size of  $224 \times 224$  pixels which matches image size commonly used in pre-trained models. Furthermore, the dataset comes with pre-made splits to ensure ease of use and standardized benchmarking. We meticulously preprocessed the data and release a user-friendly Python package [33] to directly load images for use in PyTorch.

This makes MedIMeta exceptionally accessible to ML researchers. This ease of access to a diverse set of realistic medical tasks with no need for additional preprocessing can serve as a bridge between medical professionals and the ML community, fostering interdisciplinary collaboration. Moreover, MedIMeta is an ideal platform for investigating cross-domain few-shot learning in medical imaging. The rich array of tasks and domains presents an excellent opportunity to study and develop cross-domain few-shot learning techniques.

In addition to presenting the meta-dataset, this paper also presents a technical validation of MedIMeta, demonstrating its utility through fully supervised and CD-FSL baselines. The validation confirms the dataset’s reliability and robustness, establishing it as a credible benchmark for research in ML for medical image analysis.

## Related datasets

Existing meta-datasets can be divided into two categories: those consisting of multiple datasets from a single domain, and those comprising data from multiple domains. An overview is shown in Table 1.

### *Single-domain meta-datasets*

Single domain meta-datasets offer an easy way to benchmark few-shot learning techniques such as meta-learning. One of the first meta-datasets in this category was Omniglot [18], which consists of handwritten characters from a wide range of alphabets. More challenging meta-datasets derived from natural images were obtained by subsampling the widely used ImageNet [26], or CIFAR datasets [16]. Examples include the MiniImageNet [30] and the TieredImageNet [25] datasets, as well as CIFAR-FS [2] and FC100 [22].

### *Multi-domain meta-datasets*

While single-domain meta-datasets offer an easy standardized way to evaluate few-shot learning techniques they often lack realism. In reality data are rarely from a single domain in FSL problems. This realization has led to the release of several multi-domain meta-datasets.

The visual decathlon dataset [24] is one of the first multi-domain datasets. It consists of 10 datasets from different visual tasks including traffic sign and flower recognition. It also includes Omniglot [18] and CIFAR [16] datasets discussed earlier.

Later Triantafillou et al. released another collection of 10 datasets coined the “Meta-Dataset” [27]. While it partially overlaps with the visual decathlon dataset, the “Meta-Dataset” was specifically designed to benchmark few-shot learning algorithms on multiple domains. However, it does not contain any medical datasets.

With a similar motivation Zhai et al. released the Visual Task Adaptation Benchmark (VTAB) [40]. This meta-dataset consists of 19 tasks, again, partially subsuming the previous datasets. A particular property of the VTAB benchmark is the

**Table 1.** Comparison of different datasets

Name	# domains	# datasets	# medical datasets	task types *	# tasks	# images	image size	multi-domain	different task types	multi-task	contains medical data	uniform image size
Omniglot [18]	1	1	0	MC	1	32 000	$105 \times 105$	-	-	-	-	✓
<i>mini</i> ImageNet [30]	1	1	0	MC	1	60 000	$84 \times 84$	-	-	-	-	✓
<i>tiered</i> ImageNet [25]	1	1	0	MC	1	779 165	$84 \times 84$ **	-	-	-	-	✓
CIFAR-FS [2]	1	1	0	MC	1	60 000	$32 \times 32$	-	-	-	-	✓
FC100 [22]	1	1	0	MC	1	60 000	$32 \times 32$	-	-	-	-	✓
Visual Decathlon [24]	1	10	0	MC, (B)	10	1 580 558	$\min(h, w) = 72$	✓	-	-	-	~
Meta-Dataset [27]	7	10	0	MC, (B)	10	53 068 000		✓	-	-	-	-
VTAB [40]	3	19	1	MC, (B)	19	2 244 000		✓	-	-	~	-
Meta-Album <i>Mini</i> [29]	10	40	2	MC	40	220 950	$128 \times 128$	✓	-	-	~	✓
MedMNIST v2 (2D) [39]	9	12	12	MC, B, ML, O	12	708 069	$28 \times 28$	✓	✓	-	✓	✓
<b>MedIMeta</b> (ours)	10	19	19	MC, B, ML, O	54	399 742	$224 \times 224$	✓	✓	✓	✓	✓

\* MC: multi-class, B: binary, ML: multi-label, O: ordinal. Brackets indicate that a task can be interpreted as that task type but is not defined as such in the respective benchmark dataset.

\*\* default settings.

inclusion of datasets from three different domains covering natural image understanding, structured scene understanding, and specialized tasks. The VTAB dataset is also to our knowledge the first meta-dataset to include medical images.

Dumoulin et al. [7] later unified VTAB [40] and Meta-Dataset [27] into a larger Few-Shot Classification Benchmark. Guo et al. [10] collected multiple previously available datasets from multiple domains for benchmarking CD-FSL methods. Meta-Album [29] is a collection of 40 different dataset from multiple domains and follows a similar goal to our work. While it contains more datasets than MedIMeta, it does not contain any medical domains except for microscopy.

MedMNISTv2 [39] is a collection of 12 medical imaging datasets from 9 different domains. It additionally contains 3D datasets. It is similar in spirit to our work, but we go significantly beyond MedMNIST in the number of tasks and task realism. The images in MedMNISTv2 have a very low resolution of  $28 \times 28$  pixels that obscures fine details that may be clinically relevant. In contrast, we process all images at high resolution and make them available with an image size of  $224 \times 224$  pixels, which allows to detect more clinically relevant features and is the typical resolution used in pretrained neural networks. Additionally, MedMNISTv2 does not contain any multitask datasets. In contrast, MedIMeta contains a wide variety of tasks including binary, multi-class, and multi-label classification as well as ordinal regression.

In some of the overlapping datasets, we found significant problems with MedMNIST’s preprocessing, which we improve upon. Specifically, we found that some of the center-cropped images in MedMNIST had their relevant part, i.e., the part of the image showing the disease, cropped away. We fix this problem by instead zero-padding these datasets. Additionally, some datasets in MedMNISTv2 may have training-test splits that put images of the same subject in multiple splits. We instead generated splits by taking subject information into account.

While Meta-Dataset, VTAB, Meta-Album and MedMNIST contain different domains, only VTAB and MedMNIST contain a variety of different tasks. MedIMeta is the only data collection which contains datasets with multiple tasks, providing users of MedIMeta with the option to train multi-task algorithms. Out of these benchmarks, only MedMNIST contains a significant number of *medical* tasks. Our proposed MedIMeta contains 54 medical tasks and is easily extensible to tasks from other fields, like natural images. Furthermore, we provide utilities for converting other datasets (e.g. ImageNet) into the MedIMeta format allowing to easily integrate MedIMeta with other data sources.

## Methods

We release the MedIMeta dataset, a novel, highly standardized meta-dataset comprised of 19 publicly available datasets containing a total of 54 tasks. In the following, we describe the source datasets and the data generation in detail.

### Dataset

All datasets included in the MedIMeta dataset have either been previously published under an open license that allows redistribution under a CC-BY-SA or CC-BY-SA-NC license, or we obtained an explicit permission to do so. In addition to

having an open license, we selected these datasets based on three criteria: suitability for defining a minimum of one classification task on the data, image size suitable for rescaling to our target size without producing noticeable artifacts, and a minimum of 100 images. All images in MedIMeta were standardized to an image size of  $224 \times 224$  pixels. We provide pre-defined training, validation and testing splits for all 19 datasets. If data splits were already defined in the source data, we used the pre-existing splits. Otherwise we generated our own. Most datasets include more than one classification task. Typically, there is one main diagnostic task and several auxiliary tasks. Most of these tasks were already present in the source datasets. In some instances, we created additional tasks not present in the source data. Table 2 gives an overview of all dataset, tasks, and their key properties. In the following, we describe in detail all datasets that MedIMeta is comprised of using the `dataset ID`, as well as the full dataset name.

**aml, AML Cytomorphology:** Morphological dataset of leukocytes with expert-labeled single-cell images from peripheral blood smears of patients with acute myeloid leukemia (AML) and patients without signs of hematological malignancy, derived from the *Munich AML Morphology Dataset* [21]. The 18,365 original images were resized to  $224 \times 224$  pixels using bi-cubic interpolation (no images were up-scaled) and converted to RGB format by removing the transparency channel. We adopted the original multi-class classification task with 15 morphological classes from the source dataset.

**bus, Breast Ultrasound:** Dataset of breast ultrasound images of women between 25 and 75 years old, derived from the *Breast Ultrasound Images Dataset* [6]. The 780 original images were converted to grayscale and their masks to binary format. Images and masks were zero-padded to a square shape and resized to  $224 \times 224$  pixels using bi-cubic interpolation and nearest neighbor interpolation respectively (no images were up-scaled). The multi-class tumor classification task with normal, benign, and malignant examples was adopted without modifications from the source dataset. We additionally defined a binary classification task between malignant tumors and other images.

**crc, Colorectal Cancer:** Dataset of image patches from hematoxylin & eosin (H&E) stained histological images of human colorectal cancer (CRC) and healthy tissue, derived from the *NCT-CRC-HE-100K* and *CRC-VAL-HE-7K* datasets [12]. The 107,180 original images from the training and validation sets were not modified, as they already had the right shape and size for MedIMeta. We adopted the multi-class tissue classification task with 9 labels from the source dataset without modifications.

**cxr, Chest X-ray Multi-disease:** Dataset of frontal-view X-ray chest images, derived from the *ChestX-ray14* dataset [31]. The 112,120 original images were resized to  $224 \times 224$  pixels using bi-cubic interpolation (no images were up-scaled); the 519 images that were originally in RGBA format were converted to grayscale. We provide a multi-label thorax disease classification task with 14 labels adopted without modifications from the source dataset. We additionally provide a binary classification task of the patient sex derived from the labels present in the original data.

**derm, Dermatoscopy:** Dataset of dermatoscopic images of common pigmented skin lesions from different populations acquired and stored by different modalities, derived from the *HAM10000* dataset [28]. The 11,720 original images were center-cropped to a square shape and resized to  $224 \times 224$  pixels using bi-cubic interpolation (no images were up-scaled). We provide the multi-class disease classification task with 7 labels defined in the challenge hosted by the International Skin Imaging Collaboration (ISIC) [4].

**dr\_regular, Diabetic Retinopathy (Regular Fundus):** Dataset of fundus images with diabetic retinopathy grades and image quality annotations, derived from the *DeepDRiD* dataset [20]. The 2,000 original images were center-cropped to a square shape and resized to  $224 \times 224$  pixels using bi-cubic interpolation (no images were up-scaled). Following the annotations present in the original data, we provide 5 tasks: diabetic retinopathy grade (ordinal regression task with 5 labels), sufficient image quality for gradability (binary classification task), strength of artifact (ordinal regression task with 6 labels), image clarity (ordinal regression task with 5 labels), and field definition (ordinal regression task with 5 labels).

**dr\_uwf, Diabetic Retinopathy (Ultra-widefield Fundus):** Dataset of ultra-widefield fundus images with annotations for diabetic retinopathy grading, derived from the *DeepDRiD* dataset [20]. Only the 250 original images without missing labels were kept. They were center-cropped to a square shape and resized to  $224 \times 224$  pixels using bi-cubic interpolation (no images were up-scaled). We adopted the DR grading task (ordinal regression) with 5 labels from the source dataset without modifications.

**fundus, Fundus Multi-disease:** Multi-disease retinal fundus dataset of images captured using three different fundus cameras with 45 conditions annotated through adjudicated consensus of two senior retinal experts as well as an overall disease presence label, derived from the *Retinal Fundus Multi-disease Image Dataset* [23]. The 3,200 images were center-cropped

to a square shape and resized to  $224 \times 224$  pixels using bi-cubic interpolation (no images were up-scaled). The original disease presence binary classification task and disease multi-label classification task with 45 labels were directly derived from the annotations provided by the original dataset.

**glaucoma, Glaucoma-specific fundus images:** Glaucoma-specific Indian ethnicity retinal fundus dataset of images acquired using three devices, where five expert ophthalmologists provided annotations on whether the subject is suspect for glaucoma or not, derived from the *Chákṣu* dataset [17]. The 1,345 original images and their masks were zero-padded to a square shape and resized to  $224 \times 224$  pixels using bi-cubic interpolation and nearest neighbor interpolation respectively (no images were up-scaled). We used the glaucoma suspect majority vote annotation to derive a binary classification task.

**mammo\_calc, Mammography (Calcifications):** Dataset of cropped regions of interest (calcifications), derived from the *Curated Breast Imaging Subset of the Digital Database for Screening Mammography* (CBIS-DDSM) [19]. The 1,872 images were obtained by extending the regions of interest (bounding boxes) to a square shape with a minimum size of  $224 \times 224$  pixels, and extracting the resulting region crops from the full original images. The region crops were then resized to  $224 \times 224$  pixels using bi-cubic interpolation. From the annotations, 3 tasks were derived: pathology presence (binary classification task), calcification type (multi-label classification task with 14 labels), and calcification distribution (multi-label classification task with 5 labels).

**mammo\_mass, Mammography (Masses):** Dataset of cropped regions of interest (masses) from CBIS-DDSM. The 1,696 images were preprocessed as described for *Mammography (Calcifications)*. From the annotations, 3 tasks were derived: pathology presence (binary classification task), mass shape (multi-label classification task with 8 labels), and mass margins (multi-label classification task with 5 labels).

**oct, OCT:** Dataset of validated Optical Coherence Tomography (OCT) images labeled for disease classification, derived from [14]. The 84,484 original images were center-cropped to a square shape and resized to  $224 \times 224$  pixels using bi-cubic interpolation (no images were up-scaled). The original dataset contains a multi-class disease classification task, with three different diseases and a healthy class, which we adopt without modifications. Additionally, we provide a binary task for whether the image warrants urgent referral to a specialist based on the annotations present in the original data.

**organs\_axial, Axial Organ Slices:** Dataset of axial image slices of 11 different organs, extracted from the *Liver Tumor Segmentation Benchmark* (LiTS) dataset [3] and the corresponding organ bounding box annotations from [38]. We derived a multi-class organ classification task with 11 labels by extracting a cropped image of each individual organ in each of the CT volumes using the bounding box annotations. We obtained a total of 1,645 organ images. We removed 106 images for which the voxel size information was missing. The axes on one image were permuted to bring it to the same format as the other images. The images and masks were sliced from the original 3D volumes by taking the center of the organ bounding box in the axial plane. The Hounsfield-Units of the images were transformed into grayscale images by applying a window with a width of 400 and a level of 50, which are typical values for abdominal CT imaging. The images and masks were cropped to a square size in the physical space, by centering at the center of the bounding box and expanding the smaller side. The resulting images and masks were resized to  $224 \times 224$  pixels using bi-cubic and nearest neighbor interpolation, respectively. For visualization purposes, we additionally provide images averaged over the 10% central slices with the projected bounding boxes of all organs extracted from the image drawn on top.

**organs\_coronal, Coronal Organ Slices:** Dataset of coronal image slices of 11 different organs, extracted from the LiTS dataset. The images were processed the same as described for the *Axial Organ Slices* dataset, except that the coronal projections were used.

**organs\_sagittal, Sagittal Organ Slices:** Dataset of sagittal image slices of 11 different organs, extracted from the LiTS dataset. The images were processed the same as described for the *Axial Organ Slices* dataset, except that the sagittal projections were used.

**pbcc, Peripheral Blood Cells:** Dataset of microscopic peripheral blood cell images of individual normal cells, captured from individuals without infection, with hematologic or oncologic disease and free of any pharmacologic treatment at the moment of blood collection, derived from [1]. The 17,092 original images were center-cropped to a square shape and resized to  $224 \times 224$  pixels using bi-cubic interpolation (no images were up-scaled). We adopted the original multi-class blood cell classification task with 8 labels from the source dataset without modifications to the annotations.

**pneumonia, Pediatric Pneumonia:** Dataset of pediatric chest X-ray images labeled for pneumonia classification, derived from [14]. The 5,856 original images were zero-padded to a square shape and resized to  $224 \times 224$  pixels using bi-cubic interpolation (some images were up-scaled); the 283 images that were originally in RGB format were converted to

grayscale. From the original annotations, we derived a binary classification task for pneumonia presence as well as a multi-class task differentiating between normal images, bacterial pneumonia and viral pneumonia.

**skin1\_photo, Skin Lesion Evaluation (Clinical Photography):** A dataset containing clinical color photography images of skin lesions, along with corresponding labels for seven different evaluation criteria and the diagnosis, derived from [13]. The images were zero-padded to obtain a square image and then resized to  $224 \times 224$  pixels using bi-cubic interpolation. We adopted an overall diagnostic multi-class task, as well as separate classification tasks for each of the seven diagnostic criteria from the source dataset. Tasks containing infrequent labels have additional grouped versions which bundle the infrequent labels together into more frequent labels. This grouping is provided by the source dataset.

**skin1\_dermm, Skin Lesion Evaluation (Dermoscopy):** A dataset containing dermoscopic color images of skin lesions, along with corresponding labels for seven different evaluation criteria and the diagnosis, derived from [13]. This dataset contains the same subjects as Skin Lesion Evaluation (Clinical Photography) and images were preprocessed in the same manner. The tasks were also identical to Skin Lesion Evaluation (Clinical Photography).

We open-source all code for creating the above datasets from their respective source materials [36]. Our published source code contains easy-to-use utility functions to extend MedIMeta with additional datasets. As examples, we provide several additional pipelines to create more datasets in the same format from other medical data which is publicly available but is not published under a license which allows redistribution of derivative work.

### Python package

We release a Python package called `medimeta` that enables data loading. This package is installable via `pip install medimeta`. Users can load data as single datasets or as cross-domain batches. It also supports loading few-shot tasks with support and query sets. Additionally, it is fully compatible with TorchCross [34], a library for cross-domain and few-shot learning.

### Data Records

We have organized and made available the data files of the MedIMeta dataset on Zenodo in [37]. The data for all datasets within MedIMeta can be accessed via the provided DOI. Each dataset is packaged in a single zip file for convenience and can be downloaded either separately or in one batch with all datasets.

Each zip file contains a structured and organized collection of data, designed to facilitate ease of use and comprehensive understanding of the dataset. The content of these zip files is as follows:

**images** This folder contains all the image files for the dataset as uint8 TIFFs, named sequentially (e.g., `000000.tiff`, `000001.tiff`, etc.), ensuring easy access and exploration for human viewers.

**splits** This directory includes text files (`train.txt`, `val.txt`, and `test.txt`) listing the image paths belonging to each respective split.

**original\_splits** For source datasets with pre-existing split definitions, this directory contains those original splits, allowing users to adhere to the original data segmentation if desired. The format is the same as in the `splits` directory.

**task\_labels** Each task within the dataset is accompanied by an `.npy` file named with the respective task's name (e.g., `task_name_1.npy`, `task_name_2.npy`, etc.) contained in this folder. Each `.npy` file contains a single NumPy array that represents the labels associated with that specific task.

**annotations.csv** This file provides a comprehensive set of annotations, such as the patient id or imaging plane, for the images in the dataset, offering detailed insights and data points for those interested. It also contains all task labels to make them more readily accessible to human readers.

**images.hdf5** This file contains all the images from the folder `images` formatted as a single dataset with dimensions  $N \times C \times H \times W$ , where  $N$  represents the number of images,  $C$  the number of channels,  $H$  the height, and  $W$  the width. The HDF5 file is useful for reading data in machine learning applications.

**info.yaml** This file contains all relevant information about the dataset, including its ID, name and description, the number of images in each split, domain identifier, task definitions, and attribution information.

**LICENSE** Each dataset is accompanied by its specific license file.

**Table 2.** All MedIMeta tasks.

Dataset Name	Domain	# Train Images	# Val Images	# Test Images	Task Name	Task Target	# Labels
AML Cytomorphology	Microscopy	12 855	1 836	3 674	morphological class	multi-class classification	15
Breast Ultrasound	Breast ultrasound	546	78	156	case category malignancy	multi-class classification binary classification	3 2
Colorectal Cancer Histopathology	Histopathology	85 000	15 000	7 180	tissue class	multi-class classification	9
Chest X-ray Multi-disease	Chest X-ray	73 421	13 103	25 596	disease labels patient sex	multi-label classification binary classification	14 2
Dermatoscopy	Dermatoscopy	10 015	193	1 512	disease category	multi-class classification	7
Diabetic Retinopathy (Regular Fundus)	Retinal fundus	1 200	400	400	DR level Overall quality Artifact Clarity Field definition	ordinal regression binary classification ordinal regression ordinal regression ordinal regression	5 2 6 5 5
Diabetic Retinopathy (Ultra-widefield Fundus)	Retinal fundus	150	50	50	DR level	ordinal regression	5
Fundus Multi-disease	Retinal fundus	1 920	640	640	disease presence disease labels	binary classification multi-label classification	2 45
Glaucoma-specific fundus images	Retinal fundus	857	152	336	Glaucoma suspect	binary classification	2
Mammography (Calcifications)	Mammography	1 332	214	326	pathology calc type calc distribution	binary classification multi-label classification multi-label classification	2 14 5
Mammography (Masses)	Mammography	1 126	192	378	pathology mass shape mass margins	binary classification multi-label classification multi-label classification	2 8 5
OCT	OCT	91 615	16 694	1 000	disease class urgent referral	multi-class classification binary classification	4 2
Axial Organ Slices	Abdominal CT	871	156	618	organ label	multi-class classification	11
Coronal Organ Slices	Abdominal CT	871	156	618	organ label	multi-class classification	11
Sagittal Organ Slices	Abdominal CT	871	156	618	organ label	multi-class classification	11
Peripheral Blood Cells	Microscopy	11 964	1 709	3 419	cell class	multi-class classification	8
Pediatric Pneumonia	Chest X-ray	4 415	817	624	pneumonia presence disease class	binary classification multi-class classification	2 3
Skin Lesion Evaluation (Clinical)	Clinical skin imaging	413	203	395	Diagnosis	multi-class classification	15
					Diagnosis grouped	multi-class classification	5
					Pigment Network	multi-class classification	3
					Blue Whitish Veil	binary classification	2
					Vascular Structures	multi-class classification	8
					Vascular Structures grouped	multi-class classification	3
					Pigmentation	multi-class classification	5
					Pigmentation grouped	multi-class classification	3
					Streaks	multi-class classification	3
					Dots and Globules	multi-class classification	3
Regression Structures	multi-class classification	4					
Regression Structures grouped	binary classification	2					
Skin Lesion Evaluation (Dermoscopy)	Dermatoscopy	413	203	395	Diagnosis	multi-class classification	15
					Diagnosis grouped	multi-class classification	5
					Pigment Network	multi-class classification	3
					Blue Whitish Veil	binary classification	2
					Vascular Structures	multi-class classification	8
					Vascular Structures grouped	multi-class classification	3
					Pigmentation	multi-class classification	5
					Pigmentation grouped	multi-class classification	3
					Streaks	multi-class classification	3
					Dots and Globules	multi-class classification	3
Regression Structures	multi-class classification	4					
Regression Structures grouped	binary classification	2					

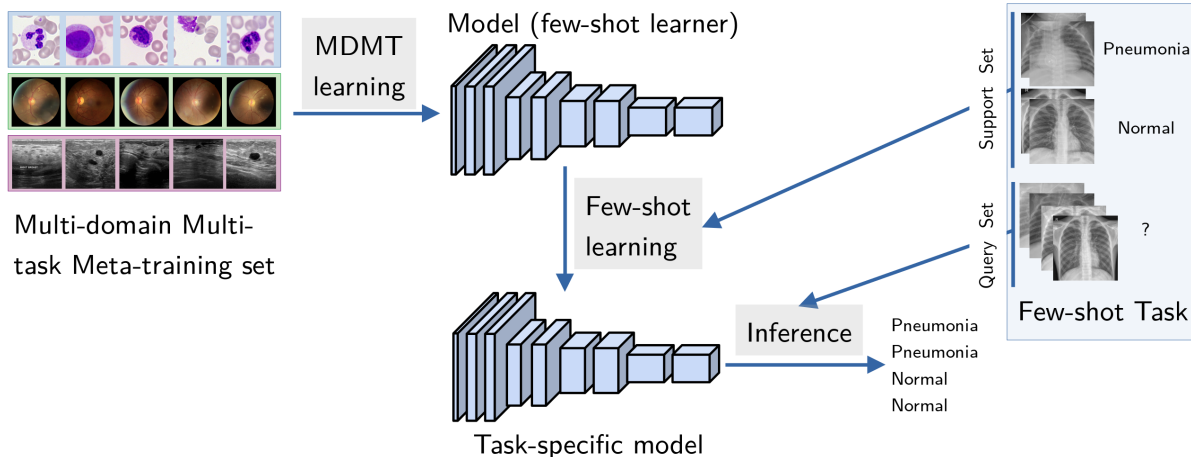


**Figure 2.** An overview of the CD-FSL scenario: The few-shot learner is first trained on the meta-dataset of highly diverse training data. It is then adapted to a new task from a new domain using the labeled examples from the support set of a few-shot task. Performance is assessed using a query set from the same task.

## Technical Validation

In order to validate our proposed dataset, we used it in two distinct learning scenarios. First, we performed simple supervised training on each of the datasets on its primary tasks. Secondly, we investigated the utility of our dataset for CD-FSL. In the following, we describe the experiment setups for the two scenarios in more detail.

### Supervised learning experiments

For the supervised experiments we trained ResNet-18 and ResNet-50 models [11] on the primary task for each dataset. All networks were initialized with pre-trained weights from ImageNet [26]. Early stopping was performed using the AUROC on the respective validation sets.

### Cross-domain few-shot learning (CD-FSL) experiments

In this evaluation, we compare 5-shot performance using three different CD-FSL approaches (described below). We evaluated the performance for each dataset in a leave-one-out fashion using one task as target task, and the other tasks from all datasets with no domain overlap or subject overlap as source tasks to transfer knowledge from. The knowledge transfer was achieved by first training a common backbone on the source tasks, and then fine-tuning the network to the target task using a small support set of 5 labeled examples per class. Evaluation was performed on a distinct query set consisting of 10 samples from the same task. Figure 2 illustrates the training and evaluation procedure. Because performance can vary substantially between runs due to the quality of the 5 labeled examples, we reran the experiments 100 times for each target task to obtain a more robust estimation of the performance.

#### Baseline CD-FSL algorithms

**ImageNet pre-training (IM-PT):** The simplest baseline we investigated is simply initializing the common backbone network with ImageNet weights, and then directly fine-tuning to the target task.

**Multi-domain multi-task pre-training (mm-PT):** Pre-training using ImageNet lacks specificity to the medical domain. Incrementally pre-training on a series of available datasets may offer a strategy to learn from many related datasets rather than just one [5]. However, incremental pre-training may suffer from catastrophic forgetting of earlier tasks [15]. To address this issue, we propose a multi-domain multi-task pre-training schedule, where for each model update we sample a batch from a random source task. This strategy may facilitate learning representations suitable for a wide range of tasks. The algorithm is summarized in the supplemental materials.

**Multi-domain Multi-task MAML (mm-MAML):** Model-agnostic meta-learning [8] has been shown to be a promising strategy for CD-FSL [9]. MAML first “learns to learn” from a set of training tasks before learning the desired test task. However, MAML assumes identical task types and number of classes for each task, which is not realistic in practical settings. Here, we employed our previously proposed Multi-domain Multi-task MAML (mm-MAML) strategy [35] where we used an individual classification layer for each class that is simply initialized with zeros. The algorithm is summarized in the supplemental materials.

## Results

Table 3 shows the results for the single-domain baselines. It can be seen that the models were able to achieve a high performances in terms of AUROC for most datasets. The comparatively low performance on the diabetic retinopathy detection from ultra-wide field images (dr\_uwf) reflects the difficulty of the task. As expected, the more complex ResNet 50 model achieved slightly higher performance for most datasets compared to the ResNet 18.

**Table 3.** AUROC (%) on the test set for the fully supervised baselines.

	aml	bus	crc	cxr	derm	dr_ regular	dr_ uwf	fundus	glaucoma	mammo_ calc
ResNet 18	<b>99.1</b>	96.0	<b>99.5</b>	78.4	94.0	84.9	58.1	97.1	74.5	<b>76.8</b>
ResNet 50	98.4	<b>96.6</b>	<b>99.5</b>	<b>80.5</b>	<b>96.2</b>	<b>86.5</b>	<b>58.3</b>	<b>97.2</b>	<b>86.6</b>	75.0

	mammo_ mass	oct	organs_ axial	organs_ coronal	organs_ sagittal	pbc	pneumonia	skin_ photo	skin_ derm
ResNet 18	<b>73.0</b>	99.7	97.8	97.1	96.7	99.9	98.7	75.0	82.9
ResNet 50	72.3	<b>99.8</b>	<b>98.6</b>	<b>97.9</b>	<b>96.8</b>	<b>100.0</b>	<b>99.3</b>	<b>78.0</b>	<b>90.1</b>

**Table 4.** AUROC (%) for the CD-FSL baselines averaged across 100 5-shot episodes using a ResNet18 and ResNet50.

Training Type	Backbone	aml	bus	crc	cxr	derm	dr_ regular	dr_ uwf	fundus	glaucoma	mammo_ calc
ImageNet	ResNet18	<b>82.1 ± 0.6</b>	71.4 ± 1.8	94.2 ± 0.4	<b>58.5 ± 0.6</b>	74.4 ± 1.0	69.4 ± 1.1	53.0 ± 1.6	75.1 ± 2.6	55.0 ± 2.9	61.4 ± 2.6
	ResNet50	82.0 ± 0.7	<b>72.9 ± 1.7</b>	<b>95.4 ± 0.3</b>	57.9 ± 0.6	<b>74.9 ± 0.8</b>	<b>71.3 ± 0.9</b>	<b>54.0 ± 1.6</b>	<b>77.0 ± 2.4</b>	53.0 ± 2.8	<b>64.2 ± 2.8</b>
MM-PFT	ResNet18	77.9 ± 0.8	66.2 ± 1.7	85.8 ± 0.6	55.5 ± 0.5	69.7 ± 0.8	65.1 ± 1.1	51.2 ± 1.5	64.2 ± 2.9	<b>56.2 ± 3.1</b>	60.5 ± 2.8
	ResNet50	79.6 ± 0.7	69.7 ± 1.7	89.7 ± 0.5	57.1 ± 0.6	72.1 ± 1.0	67.9 ± 1.0	52.3 ± 1.6	69.8 ± 2.5	53.4 ± 2.6	60.1 ± 3.1
MM-MAML	ResNet18	70.3 ± 0.7	61.5 ± 1.8	82.4 ± 0.6	54.4 ± 0.5	68.6 ± 0.8	63.3 ± 1.1	51.1 ± 1.5	58.4 ± 2.8	52.2 ± 2.8	58.3 ± 2.8

Training Type	Backbone	mammo_ mass	oct	organs_ axial	organs_ coronal	organs_ sagittal	pbc	pneumonia	skin_ photo	skin_ derm
ImageNet	ResNet18	54.3 ± 3.0	73.0 ± 1.2	<b>96.5 ± 0.3</b>	<b>92.9 ± 0.4</b>	<b>89.0 ± 0.5</b>	89.6 ± 0.6	<b>95.3 ± 1.1</b>	60.4 ± 1.8	69.5 ± 1.7
	ResNet50	<b>55.5 ± 2.8</b>	<b>74.9 ± 1.3</b>	94.6 ± 0.3	88.8 ± 0.4	85.6 ± 0.5	<b>94.4 ± 0.5</b>	94.9 ± 1.1	60.5 ± 1.6	<b>70.8 ± 1.8</b>
MM-PFT	ResNet18	55.4 ± 2.9	68.9 ± 1.3	92.1 ± 0.3	87.0 ± 0.4	84.8 ± 0.5	85.0 ± 0.8	88.5 ± 1.8	<b>63.0 ± 1.7</b>	67.5 ± 1.8
	ResNet50	54.2 ± 3.2	67.0 ± 1.4	91.3 ± 0.4	86.9 ± 0.5	85.9 ± 0.5	88.5 ± 0.8	91.4 ± 1.6	59.7 ± 1.7	65.4 ± 1.8
MM-MAML	ResNet18	53.6 ± 2.8	63.6 ± 1.2	88.6 ± 0.4	82.4 ± 0.5	81.6 ± 0.5	83.7 ± 0.7	90.9 ± 1.4	56.6 ± 1.5	67.5 ± 1.7

Table 4 shows 5-shot results for the CD-FSL baselines described earlier. Surprisingly, simple fine-tuning from pre-trained ImageNet weights performed as well or better than fine-tuning from the two pre-fine-tuning and MAML baselines. This can mean that the pre-fine-tuning method we chose is too simple to bring a meaningful benefit. At the same time it is also apparent that simple methods for few-shot learning such as these do not achieve performance close to fully supervised training. We therefore conclude that MedIMeta offers high enough complexity for evaluating future few-shot methods, with the fully supervised results setting an upper bar for future few-shot methods to achieve.

## Usage Notes

All datasets contained in the MedIMeta dataset [37] can be downloaded from Zenodo. Using the code provided in our data loaders repository [33], all tasks in MedIMeta can easily be loaded as PyTorch datasets for single-domain, cross-domain and few-shot scenarios. No further pre-processing is required, but it is possible to provide any TorchVision transforms to the dataset class when initializing it. A simple step-by-step example of how to load a single dataset is as follows.

1. Download the zip file for the dataset you would like to use (e.g. OCT) from the Zenodo record [37], and extract it to a directory of choice. Let us use `./data/MedIMeta` here.
2. `pip install medimeta`
3. The data can now be used as a PyTorch dataset. The following code snippet would instantiate the dataset for the Disease task of the OCT dataset, assuming the data is stored in the `data/MedIMeta` directory.

```
from medimeta import MedIMeta
dataset = MedIMeta("data/MedIMeta", "oct", "Disease")
```

The repository also contains a directory “examples” which contains several usage examples for single-domain training, cross-domain training, and few-shot fine-tuning.

## Code availability

The algorithms, methodologies, and procedures used in this paper are fully documented in our accompanying code repositories. All code has been developed in Python and builds on widely used libraries. Specific dependencies and their versions are documented as requirements in the respective repositories, ensuring easy setup and reproducibility.

**MedIMeta dataset scripts:** The source code for creating datasets from their respective materials contains all scripts needed for the creation of the 19 MedIMeta datasets, utility functions for extending the MedIMeta with additional datasets and all parameters used, such as image size. Code available under [36].

**MedIMeta data loaders:** Easy-to-use code for data loading from MedIMeta is provided both for the single-domain and the cross-domain (few-shot) scenarios. The code is available at [33]. The package can be directly installed using `pip install medimeta`.

**Experiments:** The code for our experiments includes scripts for preprocessing, data augmentation, model training, evaluation, and other necessary utilities. It utilizes our data loader code described above. The code is available under [32].

**TorchCross library:** A general PyTorch few-shot learning and cross-domain learning library which is used in the MedIMeta data loaders code. The code is available under [34], and the package can be directly installed using `pip install torchcross`.

## References

- [1] Andrea Acevedo, Anna Merino, Santiago Alférez, Ángel Molina, Laura Boldú, and José Rodellar. “A dataset of microscopic peripheral blood cell images for development of automatic recognition systems”. In: *Data in Brief* 30 (June 2020), p. 105474. ISSN: 23523409. DOI: [10.1016/j.dib.2020.105474](https://doi.org/10.1016/j.dib.2020.105474). (Visited on 03/04/2023).
- [2] Luca Bertinetto, Joao F Henriques, Philip HS Torr, and Andrea Vedaldi. “Meta-learning with differentiable closed-form solvers”. In: *arXiv preprint arXiv:1805.08136* (2018).
- [3] Patrick Bilic et al. “The liver tumor segmentation benchmark (lits)”. In: *Medical Image Analysis* 84 (2023), p. 102680.
- [4] Noel Codella et al. “Skin lesion analysis toward melanoma detection 2018: A challenge hosted by the international skin imaging collaboration (isic)”. In: *arXiv preprint arXiv:1902.03368* (2019).
- [5] Guy Davidson and Michael C Mozer. “Sequential mastery of multiple visual tasks: Networks naturally learn to learn and forget to forget”. In: *Proceedings of the IEEE/CVF Conference on Computer Vision and Pattern Recognition*. 2020, pp. 9282–9293.
- [6] Walid Al-Dhabyani, Mohammed Goma, Hussien Khaled, and Aly Fahmy. “Dataset of breast ultrasound images”. In: *Data in Brief* 28 (Feb. 2020), p. 104863. ISSN: 23523409. DOI: [10.1016/j.dib.2019.104863](https://doi.org/10.1016/j.dib.2019.104863). (Visited on 03/04/2023).
- [7] Vincent Dumoulin, Neil Houlsby, Utku Evci, Xiaohua Zhai, Ross Goroshin, Sylvain Gelly, and Hugo Larochelle. *Comparing Transfer and Meta Learning Approaches on a Unified Few-Shot Classification Benchmark*. 2021. DOI: [10.48550/ARXIV.2104.02638](https://doi.org/10.48550/ARXIV.2104.02638).
- [8] Chelsea Finn, Pieter Abbeel, and Sergey Levine. “Model-Agnostic Meta-Learning for Fast Adaptation of Deep Networks”. In: *Proceedings of the 34th International Conference on Machine Learning*. Vol. 70. PMLR, June 2017, pp. 1126–1135.
- [9] Yunhui Guo, Noel C Codella, Leonid Karlinsky, James V Codella, John R Smith, Kate Saenko, Tajana Rosing, and Rogerio Feris. “A broader study of cross-domain few-shot learning”. In: *Computer Vision—ECCV 2020: 16th European Conference, Glasgow, UK, August 23–28, 2020, Proceedings, Part XXVII 16*. Springer. 2020, pp. 124–141.
- [10] Yunhui Guo, Noel C. Codella, Leonid Karlinsky, James V. Codella, John R. Smith, Kate Saenko, Tajana Rosing, and Rogerio Feris. *A Broader Study of Cross-Domain Few-Shot Learning*. 2019. DOI: [10.48550/ARXIV.1912.07200](https://doi.org/10.48550/ARXIV.1912.07200).
- [11] Kaiming He, Xiangyu Zhang, Shaoqing Ren, and Jian Sun. “Deep Residual Learning for Image Recognition”. In: *Proceedings of the IEEE Conference on Computer Vision and Pattern Recognition (CVPR)*. June 2016.

- [12] Jakob Nikolas Kather, Niels Halama, and Alexander Marx. *100,000 Histological Images Of Human Colorectal Cancer And Healthy Tissue*. Type: dataset. Apr. 7, 2018. DOI: [10.5281/ZENODO.1214456](https://doi.org/10.5281/ZENODO.1214456). URL: <https://zenodo.org/record/1214456> (visited on 03/04/2023).
- [13] Jeremy Kawahara, Sara Daneshvar, Giuseppe Argenziano, and Ghassan Hamarneh. “Seven-Point Checklist and Skin Lesion Classification Using Multitask Multimodal Neural Nets”. In: *IEEE Journal of Biomedical and Health Informatics* 23.2 (2019), pp. 538–546. DOI: [10.1109/JBHI.2018.2824327](https://doi.org/10.1109/JBHI.2018.2824327).
- [14] Daniel S. Kermany et al. “Identifying Medical Diagnoses and Treatable Diseases by Image-Based Deep Learning”. In: *Cell* 172.5 (Feb. 2018), 1122–1131.e9. ISSN: 00928674. DOI: [10.1016/j.cell.2018.02.010](https://doi.org/10.1016/j.cell.2018.02.010). (Visited on 03/04/2023).
- [15] James Kirkpatrick et al. “Overcoming catastrophic forgetting in neural networks”. In: *Proceedings of the national academy of sciences* 114.13 (2017), pp. 3521–3526.
- [16] Alex Krizhevsky. *Learning multiple layers of features from tiny images*. 2009.
- [17] JR Harish Kumar, Chandra Sekhar Seelamantula, JH Gagan, Yogish S Kamath, Neetha IR Kuzhuppilly, U Vivekanand, Preeti Gupta, and Shilpa Patil. “Chákṣu: A glaucoma specific fundus image database”. In: *Scientific data* 10.1 (2023), p. 70.
- [18] Brenden M Lake, Ruslan Salakhutdinov, and Joshua B Tenenbaum. “Human-level concept learning through probabilistic program induction”. In: *Science* 350.6266 (2015), pp. 1332–1338.
- [19] Rebecca Sawyer Lee, Francisco Gimenez, Assaf Hoogi, Kanae Kawai Miyake, Mia Gorovoy, and Daniel L. Rubin. “A curated mammography data set for use in computer-aided detection and diagnosis research”. In: *Scientific Data* 4.1 (Dec. 19, 2017), p. 170177. ISSN: 2052-4463. DOI: [10.1038/sdata.2017.177](https://doi.org/10.1038/sdata.2017.177). URL: <https://www.nature.com/articles/sdata2017177> (visited on 03/04/2023).
- [20] Ruhan Liu et al. “Deepdrid: Diabetic retinopathy—grading and image quality estimation challenge”. In: *Patterns* 3.6 (2022), p. 100512.
- [21] Christian Matek, Simone Schwarz, Karsten Spiekermann, and Carsten Marr. “Human-level recognition of blast cells in acute myeloid leukaemia with convolutional neural networks”. In: *Nature Machine Intelligence* 1.11 (Nov. 12, 2019), pp. 538–544. ISSN: 2522-5839. DOI: [10.1038/s42256-019-0101-9](https://doi.org/10.1038/s42256-019-0101-9). (Visited on 03/04/2023).
- [22] Boris Oreshkin, Pau Rodríguez López, and Alexandre Lacoste. “Tadam: Task dependent adaptive metric for improved few-shot learning”. In: *Advances in neural information processing systems* 31 (2018).
- [23] Samiksha Pachade, Prasanna Porwal, Dhanshree Thulkar, Manesh Kokare, Girish Deshmukh, Vivek Sahasrabudhe, Luca Giancardo, Gwenolé Quéllec, and Fabrice Mériaudeau. “Retinal fundus multi-disease image dataset (rfmid): A dataset for multi-disease detection research”. In: *Data* 6.2 (2021), p. 14.
- [24] Sylvestre-Alvise Rebuffi, Hakan Bilen, and Andrea Vedaldi. “Learning multiple visual domains with residual adapters”. In: *Advances in neural information processing systems* 30 (2017).
- [25] Mengye Ren, Eleni Triantafillou, Sachin Ravi, Jake Snell, Kevin Swersky, Joshua B. Tenenbaum, Hugo Larochelle, and Richard S. Zemel. *Meta-Learning for Semi-Supervised Few-Shot Classification*. 2018. arXiv: [1803.00676 \[cs.LG\]](https://arxiv.org/abs/1803.00676).
- [26] Olga Russakovsky et al. “ImageNet Large Scale Visual Recognition Challenge”. In: *International Journal of Computer Vision (IJCV)* 115.3 (2015), pp. 211–252. DOI: [10.1007/s11263-015-0816-y](https://doi.org/10.1007/s11263-015-0816-y).
- [27] Eleni Triantafillou et al. “Meta-dataset: A dataset of datasets for learning to learn from few examples”. In: *arXiv preprint arXiv:1903.03096* (2019).
- [28] Philipp Tschandl, Cliff Rosendahl, and Harald Kittler. “The HAM10000 dataset, a large collection of multi-source dermatoscopic images of common pigmented skin lesions”. In: *Scientific data* 5.1 (2018), pp. 1–9.
- [29] Ihsan Ullah et al. “Meta-Album: Multi-domain Meta-Dataset for Few-Shot Image Classification”. In: *Thirty-sixth Conference on Neural Information Processing Systems Datasets and Benchmarks Track*. 2022. URL: <https://meta-album.github.io/>.
- [30] Oriol Vinyals, Charles Blundell, Timothy Lillicrap, koray kavukcuoglu koray, and Daan Wierstra. “Matching Networks for One Shot Learning”. In: *Advances in Neural Information Processing Systems*. Ed. by D. Lee, M. Sugiyama, U. Luxburg, I. Guyon, and R. Garnett. Vol. 29. Curran Associates, Inc., 2016.

- [31] Xiaosong Wang, Yifan Peng, Le Lu, Zhiyong Lu, Mohammadhadi Bagheri, and Ronald M. Summers. “ChestX-ray8: Hospital-Scale Chest X-Ray Database and Benchmarks on Weakly-Supervised Classification and Localization of Common Thorax Diseases”. In: *Proceedings of the IEEE Conference on Computer Vision and Pattern Recognition (CVPR)*. July 2017.
- [32] Stefano Woerner. *MedIMeta Experiments*. 2024. URL: <https://github.com/StefanoWoerner/medimeta-experiments>.
- [33] Stefano Woerner. *MedIMeta for PyTorch*. 2024. URL: <https://github.com/StefanoWoerner/medimeta-pytorch>.
- [34] Stefano Woerner. *TorchCross*. 2024. URL: <https://github.com/StefanoWoerner/torchcross>.
- [35] Stefano Woerner and Christian F. Baumgartner. “Strategies for Meta-Learning with Diverse Tasks”. In: *Medical Imaging with Deep Learning*. 2022.
- [36] Stefano Woerner and Arthur Jaques. *MedIMeta Dataset Scripts*. 2024. URL: <https://github.com/StefanoWoerner/medimeta-dataset-scripts>.
- [37] Stefano Woerner, Arthur Jaques, and Christian F. Baumgartner. *A comprehensive and easy-to-use multi-domain multi-task medical imaging meta-dataset (MedIMeta)*. 2024. DOI: [10.5281/zenodo.7884735](https://doi.org/10.5281/zenodo.7884735).
- [38] Xuanang Xu, Fugen Zhou, Bo Liu, Dongshan Fu, and Xiangzhi Bai. “Efficient multiple organ localization in CT image using 3D region proposal network”. In: *IEEE transactions on medical imaging* 38.8 (2019), pp. 1885–1898.
- [39] Jiancheng Yang, Rui Shi, Donglai Wei, Zequan Liu, Lin Zhao, Bilian Ke, Hanspeter Pfister, and Bingbing Ni. “MedM-NIST v2-A large-scale lightweight benchmark for 2D and 3D biomedical image classification”. In: *Scientific Data* 10.1 (2023), p. 41.
- [40] Xiaohua Zhai et al. *A Large-scale Study of Representation Learning with the Visual Task Adaptation Benchmark*. 2019. DOI: [10.48550/ARXIV.1910.04867](https://doi.org/10.48550/ARXIV.1910.04867).

## Acknowledgements

Funded by the Deutsche Forschungsgemeinschaft (DFG, German Research Foundation) under Germany’s Excellence Strategy – EXC number 2064/1 – Project number 390727645. The authors thank the International Max Planck Research School for Intelligent Systems (IMPRS-IS) for supporting Stefano Woerner.

## Author contributions statement

SW and CB conceived the dataset and the experiments, SW and AJ pre-processed and prepared the data, SW conducted the experiments. All authors reviewed the manuscript.

## Competing interests

The authors have no competing interests to declare.

# Supplementary material for: A comprehensive and easy-to-use multi-domain multi-task medical imaging meta-dataset (MedIMeta)

Stefano Woerner<sup>1</sup>, Arthur Jaques<sup>1</sup>, and Christian F. Baumgartner<sup>1,2</sup>

<sup>1</sup>Cluster of Excellence “Machine Learning: New Perspectives for Science”, University of Tübingen, Germany

<sup>2</sup>Faculty of Health Sciences and Medicine, University of Lucerne, Switzerland

## Training Algorithms

### Multi-domain multi-task pre-training

To address the issue of catastrophic forgetting, we propose a multi-domain multi-task pre-training schedule (which we abbreviate with mm-PT), where the model is simultaneously pre-trained on all datasets in our meta-dataset. This means that the model will be simultaneously trained on multiple heterogeneous domains and tasks. To achieve this, the network is divided into a backbone and a classification head, where the last linear layer of the network is removed to create the backbone, and a linear layer is initialized as the head for each task. The algorithm for mm-PT involves randomly sampling batches from each of the tasks and training the model on these batches. The appropriate head and loss function is used for each batch, as illustrated in algorithm 1. When fine-tuning to the target task, a new head appropriate for the target task is attached to the backbone.

---

#### Algorithm 1 Multi-domain Multi-task Pre-training

---

**Require:** Set  $T$  of tasks, Datasets  $D_t$  for tasks  $t \in T$ , Model  $f$  with parameters  $\theta$ , Classification heads  $l_t$  for  $t \in T$

- 1: **while** training has not converged **do**
  - 2:      $t \leftarrow$  Sample a task  $t$  from  $T$  with probability  $\frac{|D_t|}{\sum_{j \in T} |D_j|}$
  - 3:      $B \leftarrow$  Sample a batch from dataset  $D_t$
  - 4:      $\theta \leftarrow \theta - \nabla_{\theta} \mathcal{L}_t(l_t(f(B; \theta)))$
  - 5: **end while**
  - 6: **return**  $\theta$
- 

### Multi-domain multi-task meta-learning

The appearance of medical images can vary significantly depending on the imaging modality used. Furthermore, the nature of tasks involved in medical image analysis varies considerably, encompassing a range of classifications such as binary, multi-class, or multi-label, and differing in the number of target labels or classes required.

To enable meta-learning in a multi-domain multi-task setting, we propose a simple extension of MAML [8] that can learn from a diverse set of tasks prior to fine-tuning on the target task. Although MAML can be applied to almost any neural network architecture, the assumption of a constant architecture becomes an issue when training with a set of diverse tasks: if tasks have diverse targets, at least the output layer has to change. We have investigated attaching new per-task classification layers as an extension of MAML and how to initialize them in [35]. Initialising the weights of the classification layer with zeros mitigates the performance drop experienced with the default Kaiming initialisation. We therefore use this strategy as our default initialization scheme for the task-specific classification heads. Additionally, in each episode we use the loss function which is appropriate for the respective task.

The proposed Multi-domain Multi-task MAML (mm-MAML) is trained simultaneously on all datasets in our meta-dataset by sampling few-shot tasks at random from each of the tasks and using the appropriate head and loss function. At meta-test time, i.e. when fine-tuning to the target task, a new head and loss function is simply created for each target task, exactly as described in the previous section on transfer learning. The training algorithm is described in Algorithm 2.

---

**Algorithm 2** Multi-Domain Multi-Task MAML

---

**Require:** Set  $T$  of tasks, Datasets  $D_t$  for tasks  $t \in T$ , Model  $f$  with parameters  $\theta$  and meta-parameters  $\varphi$ , The number of inner steps  $I$

```
1: while training has not converged do
2:    $t \leftarrow$  Sample a task  $t$  from  $T$ 
3:    $C \leftarrow$  Sample a set  $C$  of classes from  $\mathcal{P}(C_t)$ 
4:    $l \leftarrow$  create a classification head  $l$  for the task  $t$  with classes  $C$ 
5:    $S \leftarrow$  Sample a support set from dataset  $D_t$ 
6:    $Q \leftarrow$  Sample a query set from dataset  $D_t$ 
7:    $\theta \leftarrow \varphi$ 
8:   for  $i \in \{1 \dots I\}$  do
9:      $\theta \leftarrow \theta - \nabla_{\theta} \mathcal{L}_t(l(f(S; \theta)))$ 
10:  end for
11:   $\varphi \leftarrow \varphi - \nabla_{\varphi} \mathcal{L}_t(l(f(Q; \theta)))$ 
12: end while
13: return  $\theta$ 
```

---